TIME-RESOLVED STUDY OF DROPLET FORMATION PROCESS DURING INKJETTING OF ALGINATE SOLUTION

Changxue Xu[1], Zhengyi Zhang[2], Jianzhong Fu[3], Yong Huang[2], Roger R. Markwald[4]

[1] Department of Mechanical Engineering, Clemson University, Clemson, SC 29634
[2] Department of Mechanical and Aerospace Engineering, University of Florida, Gainesville, FL 32611
[3] Department of Mechanical Engineering, Zhejiang University, Hangzhou, Zhejiang 310027, China
[4] Department of Regenerative Medicine and Cell Biology, Medical University of South Carolina, Charleston, SC 29425

Abstract

Organ printing offers a great potential for the fabrication of three-dimensional (3D) living organs by precisely layer-by-layer placing various tissue spheroids. Such fabricated organs may replace some damaged or injured human organs, emerging as a promising solution to the problem of organ donor shortage. As one of the key enabling technologies for organ printing, inkjetting has been received much attention recently. It is of great importance to understand the jetting and droplet formation processes during the inkjetting of typical biomaterials such as alginate solution. The jetting behavior and breakup time during alginate inkjetting have been studied using a time-resolved approach, and different pinch-off behaviors are classified. The resulting knowledge will help better promote the inkjetting-based organ printing technology.

Introduction

The organ donor shortage is worsening with the growing national and international demand, especially as the organs of a longer-lived population deteriorate over time. As such, there is a critical need to create three-dimensional (3D) solid multi-material, heterogeneous living constructs to meet the demand for organ and tissue transplants. Fortunately, organ printing, a biomedical application of additive manufacturing, has emerged as a promising solution to this problem by fabricating three-dimensional (3D) living organs for transplantation based on layer-by-layer deposition technique [Mironov2009] [Riggs2011]. Various technologies have been pioneered for organ printing including inkjet printing [Boland2007] [Calvert2007] [Xu2012], extrusion deposition [Khalil2005] and laser-induced forward transfer (LIFT) [Koch2010] [Schiele2010], to name a few. Of these enabling technologies, inkjet printing has gained much attention recently because of its great advantages in terms of moderate fabrication cost, inherent flexibility, and good spatial resolution and repeatability.

There are two forms of inkjet printing, continuous inkjet (CIJ) printing and drop-on-demand (DOD) inkjet printing [Herran2012a]. DOD printing is favored due to its good controllability and less contamination. During DOD printing, droplets are generated only as required by propagating a pressure wave in a fluid filled chamber. The successful implementation of DOD printing directly affects the quality of fabricated structures as well as the fabrication efficiency, so numerous studies have devoted to understating DOD printing

analytically [Amirzadeh2013], computationally [Adams1986] [Kim2012], and experimentally [Chen2002] [Herran2012b] [Castrejon-Pita2012]. Unfortunately, the droplet formation process, in particular, the jet breakup phenomenon, which is also called pinch-off, has still not well understood.

The objective of this study is to investigate the jet breakup process during DOD printing of sodium alginate solution which is a representative biomaterial commonly used in organ printing studies [Nishiyama2009] [Xu2012]. Better understanding of the formation of alginate droplets during DOD printing provides enabling technologies for various organ printing applications.

Materials and method

Materials

Alginate, particularly, sodium alginate, has been commonly used as a constituent of bioink in organ printing studies [Nishiyama2009] [Xu2012]. While alginate is not an ideal material for living tissue construction, it is a good hydrogel material for proof-of-concept studies as a viscoelastic fluid. In this study, sodium alginate (NaAlg) solutions with different concentrations were used during DOD printing. The NaAlg solutions were prepared by dissolving the sodium alginate (Sigma-Aldrich, St. Louis, MO) into deionized (di) water to make the final NaAlg solutions with the concentrations of 0.15%, 0.20%, 0.25%, 1%, 1.5% and 2% (w/v).
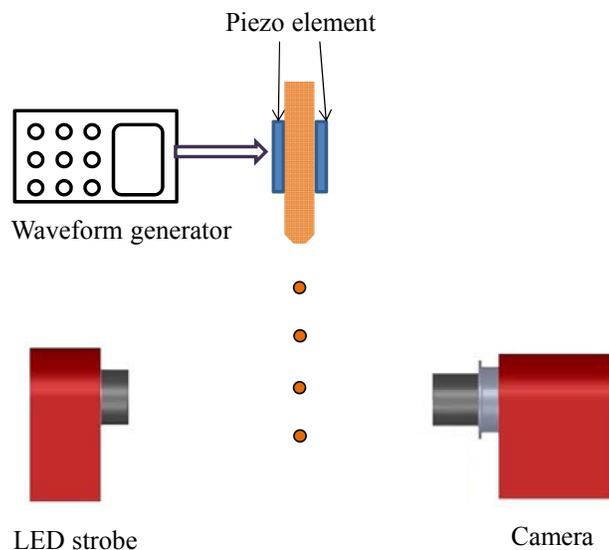
Fig. 1. Experimental setup

Method

The DOD printing system in the study was composed of three key parts: a MicroFab nozzle dispenser with a 120 μm orifice and its associated MicroFab Jet Driver, a pneumatic controller, and an imaging system. Excitation voltage was applied to the piezoelectric actuator to squeeze the nozzle, generating a pressure wave to eject the fluid out from the MicroFab nozzle dispenser to form droplets in a DOD mode. The excitation was controlled using the MicroFab Jet

Driver, and a pneumatic controller was used to adjust the back pressure of the fluid reservoir to obtain an ideal meniscus for good droplet formation. The droplet formation process was captured by the JetXpert imaging system (ImageXpert Inc., Nashua, NH), and the breakup time was measured from the captured pictures taken by using the imaging system.

Generally speaking, an external excitation voltage was applied to the dispenser to form droplets. The excitation waveform used herein was a typical bipolar waveform which consists of a succession of two square-wave pluses: either positive/negative or negative/positive [Herran2012a]. For the bipolar waveform, the second pulse of the wave is used to cancel some of residual acoustic oscillations that may remain in the dispensing nozzle after droplet ejection. The bipolar excitation waveforms applied was designed as follows [Herran2012a]: excitation voltages in the range from 40V to 70V with an interval of 5 V, voltage rise and fall times 3 µs, dwell time 30 µs, and echo time 30 µs. The experimental conditions are summarized in Table 1.

Table 1. Experimental conditions

Experimental parameters	Values
Excitation voltage (V)	40, 45, 50, 55, 60, 65, 70
Voltage rise and fall times (µs)	3
Dwell time (µs)	30
Echo time (µs)	30
Excitation frequency (Hz)	50

Results

Typical droplet formation process

Herein the droplet formation process of NaAlg solutions was studied using a time-resolved approach. Fig. 2 shows typical droplet formation processes when 0.15% and 1% NaAlg solutions were printed under an excitation voltage of 50 V, and Fig. 3 illustrates some key features defining a forming droplet. Once ejected from the nozzle, the NaAlg solution first formed a liquid jet which was a ligament with a front head. For the 0.15% NaAlg solution, the head pinched off from the ligament which was still connected to the nozzle at 95 µs, and this moment is called the (first) breakup or pinch-off time. Eventually, several other droplets formed in addition to the droplet formed first. For the 1% NaAlg solution, the ligament pinched off from the nozzle at 230 µs for the first time, and eventually the ligament either merged forward into the front head as seen in Fig. 2(b) or further broke into several satellite droplets.

0   20   50   95   135   155 (µs)

(a)

0   20   50 100 230 235 250 300 350 455 (µs)
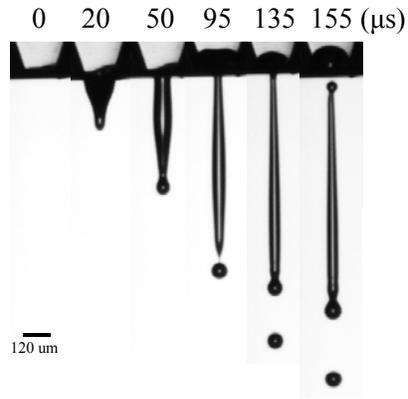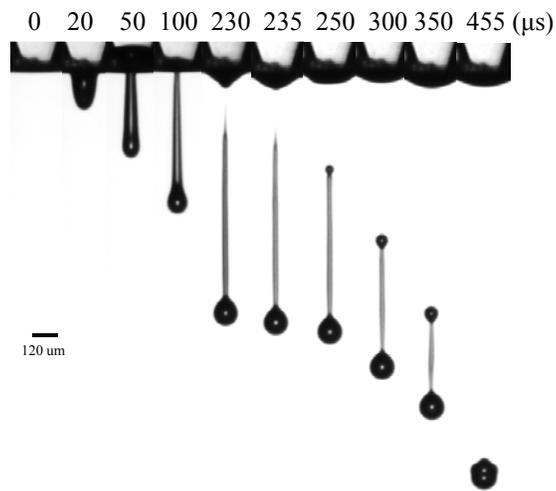
(b)

Fig. 2. Two typical droplet formation processes: (a) 0.15% NaAlg solution and (b) 1% NaAlg solution
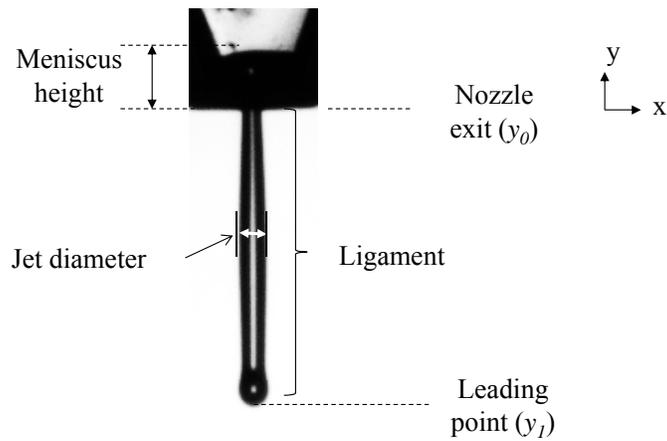
Fig. 3. Features of a forming droplet

As seen from Fig. 2, the pinch-off behavior can be quite different due to the concentration of the NaAlg solution, meaning that the droplet formation mechanism, in particular, the breakup or pinch-off process, may vary significantly. Based on the position of first breakup, two typical types of breakup have been observed: front-pinching and exit-pinching as shown in Fig. 2, respectively. During front-pinching, which is a type of end-pinching, the first breakup of liquid jet occurs near the front head. During exit-pinching, the first breakup of liquid jet occurs near the nozzle outlet. Front-pinching is commonly reported during CIJ inkjetting [Rutland1971] [Donnelly1966] while exit-pinching is more common during DOD printing [Dong2006] [Castrejon-Pita2011]. However, there is no study thus far which has reported both front-pinching and end-pinching during DOD printing.

Effect of NaAlg concentration on breakup time

NaAlg solutions with the concentrations of 0.15%, 0.20%, 0.25%, 1%, 1.5% and 2% were used to investigate the effect of NaAlg concentration on the first breakup time when the first droplet is formed. As seen from Fig. 4, the breakup time increased as the NaAlg concentration increased. This tendency is attributed to the higher viscosity, the larger elasticity, and/or the longer relaxation time of high-concentration viscoelastic NaAlg solutions. The effects of viscosity, elasticity, and relaxation time on the breakup time should be further investigated in a future study.
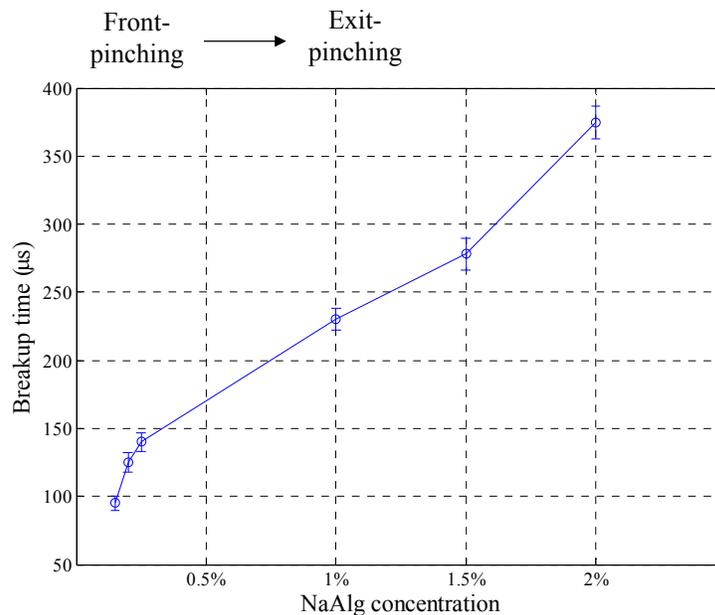
Fig. 4. Breakup time as a function of NaAlg concentration (50V)

Conclusions and future work

The jet breakup process during DOD printing of sodium alginate solution has been studied. It is found when different concentration solutions are printed, both front-pinching and end-pinching may happen. The breakup time increases with the increase of sodium alginate concentration regardless the type of pinch-off behavior. Future work may include 1) the understanding of different pinch-off mechanisms as a function of material properties and

operating conditions, and 2) the elucidation of the effects of viscosity, elasticity, and/or relaxation time on the breakup time of viscoelastic fluids.

Acknowledgement

References

[Adams1986] Adams, R.L., and Roy, J.A., 1986, "One-dimensional numerical model of a drop on demand ink-jet," Journal of Applied Mechanics, Vol. 53, pp.193-197.

[Amirzadeh2013] Amirzadeh, A., Raessi, M. and Chandra, S., 2013, "Producing molten metal droplets smaller than the nozzle diameter using a pneumatic drop-on-demand generator," Experimental Thermal and Fluid Science, Vol. 47, pp. 26-33.

[Boland2007] Boland, T., Tao, X., Damon, B.J., Manley, B., Kesari, P., Jalota, S., and Bhaduri, S., 2007, "Drop-on-demand printing of cells and materials for designer tissue constructs," Materials Science and Engineering: C, Vol. 27, pp. 372-376.

[Calvert2007] Calvert, P., 2007, "Printing cells," Nature, Vol. 318, pp. 208-209.

[Castrejon-Pita2011] Castrejon-Pita, J.R., Morrison, N.F., Harlen, O.G., Martin, G.D., and Hutchings, I.M., 2011, "Experiments and Lagrangian simulations on the formation of droplets in drop-on-demand mode," Physical Review E, Vol. 83, pp. 036306.

[Castrejon-Pita2012] Castrejon-Pita, A.A., Castrejon-Pita, J.R., and Martin, G.D., 2012, "A novel method to produce small droplets from large nozzles," Review of Scientific Instruments, Vol. 83, pp. 115105.

[Chen2002] Chen, A. U., Notz, P. K. and Basaran,O. A., 2002, "Computational and experimental analysis of pinch-off and scaling," Physical Review Letters, Vol.88, pp.174501.

[Dong2006] Dong, H., Carr, W. W., and Morris, J. F., 2006, "An experimental study of drop-on-demand drop formation," Physics of Fluids, Vol. 18, pp. 072102.

[Donnelly1966] Donnelly, R.J., and Glaberson, W., 1966, "Experiments on the capillary instability of a liquid jet," Proceedings of the Royal Society of London A, Vol. 290, pp. 547-556.

[Herran2012a] Herran, C.L., and Huang, Y., 2012, "Alginate microsphere fabrication using bipolar wave-based drop-on-demand jetting," Journal of Manufacturing Processes, Vol. 14, pp. 98-106.

[Herran2012b] Herran, C.L., Huang, Y., and Chai, W., 2012, "Performance evaluation of bipolar and tripolar excitations during nozzle-jetting-based alginate microsphere fabrication," Journal of Micromechanics and Microengineering, Vol. 22, pp. 085025.

[Khalil2005] Khalil, S., Nam, F., and Sun, W., 2005, "Multi-nozzle deposition for construction of 3D biopolymer tissue scaffolds," Rapid Prototyping Journal, Vol. 11, pp. 9-15.

[Kim2012] Kim, E., and Baek, J., 2012, "Numerical study on the effects of non-dimensional parameters on drop-on-demand droplet formation dynamics and printability range in the up-scaled model," Physics of Fluids, Vol. 24, pp. 082103.

[Koch2010] Koch, L, Kuhn, S., Sorg, H., Gruene, M., Schlie, S., Gaebel, R., Polchow, B., Reimer, K., Stoelting, S., Ma, N., Vogt, P. M., Steinhoff, G., and Chichkov, B., 2010, "Laser printing of skin cells and human stem cells," Tissue Engineering: Part C, Vol. 16, pp. 847-854.

[Mironov2009] Mironov, V., Visconti, R.P., Kasyanov, V., Forgacs, G., Drake, C.J., and Markwald, R.R., 2009, "Organ printing: tissue spheroids as building blocks," Biomaterials, Vol. 30, pp. 2164–2174.

[Nishiyama2009] Nishiyama, Y., Nakamura, M., Henmi, C., Yamaguchi, K., Mochizuki, S., Nakagawa, H., and Takiura, K., 2009, "Development of a three-dimensional bioprinter: construction of cell supporting structures using hydrogel and state-of-the-art inkjet technology," Journal of Biomechanical Engineering, Vol. 131, pp.035001.

[Riggs2011] Riggs, B.C., Dias, A.D., Schiele, N.R., Cristescu, R., Huang, Y., Corr, D.T., and Chrisey, D.B., 2011, "Matrix-assisted pulsed laser methods for biofabrication," MRS Bulletin, Vol. 36, pp. 1043-1050.

[Rutland1971] Rutland, D.F., and Jameson, G.J., 1971, "A non-linear effect in the capillary instability of liquid jets," Journal of Fluid Mechanics, Vol. 46, pp. 267-271.

[Schiele2010] Schiele, N.R., Corr, D.T., Huang, Y., Raof, N.A., Xie Y., and Chrisey, D.B., 2010, "Laser-based direct-write techniques for cell printing," Biofabrication, Vol. 2, pp. 032001.

[Xu2012] Xu, C., Chai, W., Huang, Y., and Markwald, R.R., 2012, "Scaffold-free inkjet printing of three-dimensional zigzag cellular tubes," Biotechnology and Bioengineering, Vol. 109, pp. 3152-3160.

THE INFLUENCE OF A DYNAMICALLY OPTIMIZED GALVANO BASED LASER SCANNER ON THE TOTAL SCAN TIME OF SLM PARTS

S. Buls[a], T. Craeghs[b], S. Clijsters[a], K. Kempen[a], J. Swevers[a], J.-P. Kruth[a],

[a]University of Leuven (KU Leuven), Department of Mechanical Engineering, Celestijnenlaan 300B, 3001 Heverlee, Belgium
[b]Materialise, Technologielaan 15, 3001 Leuven, Belgium

Abstract

Most commercially available Selective Laser Melting (SLM) machines use galvano based laser scanner deflection systems. This paper describes the influence of the dynamical optimization of such galvano based laser scanner on the total scan time. The system identification of a galvano laser scanner was performed in combination with the development and implementation of an optimal 'Input Shaper'. Tests were performed on lattice structured SLM parts. The process time was hereby compared, with and without the use of the optimal 'Input Shaper'. Significant scan time reduction was observed when using the optimal 'Input Shaper'.

Introduction

Selective Laser Melting (SLM) is an Additive Manufacturing technique which enables the production of complex functional metallic parts with good mechanical properties. A schematic set-up of a typical SLM machine is shown Figure 1. In the SLM process, first, a thin layer of metal powder is deposited on a build platform by means of a powder coating system. After depositing, the powder layer is melted selectively according to a predefined scanning pattern, by a laser source [1] and a laser deflection system. After scanning a layer, the build platform moves down over a fixed distance equal to the thickness of one powder layer (in SLM typically 20 to 40 µm) and a new layer is deposited and scanned. The sequence of depositing and scanning is repeated until the part(s) is (are) fully built.
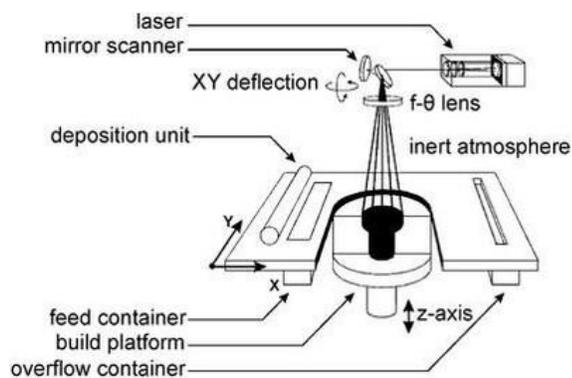
Figure 1: Schematic overview of SLM process

In recent years, the SLM technology has made an enormous progress in machine construction, production speed and part quality. Since material properties of SLM parts are nowadays comparable to the properties of the corresponding bulk material [2, 3], applications of the process can be found in domains like the medical sector [4], in tool-making industries [5–8], machine construction, aerospace, etc. However, for an even larger breakthrough of SLM in industries, which demands high quality parts and low production time and thus lower cost, the SLM process must be further time optimized.

Most commercial SLM machines available today are equipped with a galvano based laser deflection systems (galvano scanner) to deflect the laser according to the predefined scanning pattern. Throughout this paper it will be shown that the dynamical optimization of the galvano scanner plays a vital role in the reduction of the total process time.

Experimental Setup

The dynamical optimization was performed on an in-house developed SLM machine (LM-Q). This machine is fully controlled by the industrial NI-PXIe-1082 system in combination with the NI-PXI-7853R FPGA card from National Instruments. The LM-Q machine is equipped with a 300W-1064nm fiber laser and a ScanLab HurryScan25 galvano scanner.

National Instruments LabVIEW in combination with the LM-Q PXI controller was used for the dynamical measurements on the ScanLab HurryScan25 galvano scanner.

Mathworks Matlab was used for the system identification of the galvano scanner and the development of the optimal 'Input Shaper'.

Results and discussion

When scanning a SLM part, the machine controller sends a series of vectors to the galvano scanner. In essence only two types of vectors are used, namely 'jump-vectors' and 'scan-vectors'. When executing a jump-vector, the mirrors will move as fast as possible to the new coordinate without laser power, whereas when executing a scan-vector, the mirrors will move to the new coordinate with a predefined scan speed and laser power. The desired scan pattern is determined by the combination of jump- and scan-vectors.

Modern galvano scanners are designed with an optimized PID control loop to guarantee correct movement of the mirrors. This PID control loop is specifically designed for the physical properties of the galvano motors and mirrors (damping, inertia,…). However, even with the implementation of such a PID control loop, the position of the mirrors will suffer from oscillations due to the high dynamical excitation of a (fast) jump-vector. Figure 2 shows the dynamic effect of a jump-vector. The real position follows the desired position after a specific (acceleration) time. At the end of the jump-vector, the oscillations are clearly visible. To compensate for this unwanted effect a fixed delay (jump-delay) must be used (typically 750µs to 1ms) until the oscillations die out. Executing a new vector is only possible after this 'dead time'. This jump-delay results in huge time loss, mainly when manufacturing lattice structures containing a lot of very short scan vectors and where the total scan time is dominated by jump-vectors/jump-delays.
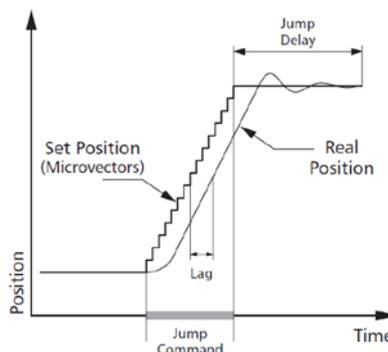
Figure 2: Jump-vector response [9]

A better solution is the use of a 'preshaping' method where all vectors are transformed in such a way that the system vibrations are kept to a minimum [10]. This can be achieved by the development of an 'Optimal Input Shaper'. When implemented, the Input Shaper will transform all the vectors before sending them to the galvano scanner. Figure 3 shows a schematic overview of the control setup. The development of the 'Input Shaper' on the LM-Q SLM machine will be further explained in the next four sections.
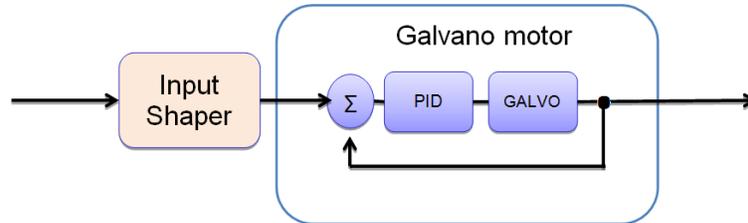
Figure 3: Schematic control overview

1. System Identification

The dynamic behavior of the galvano scanner was obtained by exciting and recording of the actual position of one of the galvano motors with a chirp signal. The excitation chirp signal has a start frequency of 10Hz and a stop frequency of 2kHz. The amplitude was set to 100bit with a measurement period of 1s. The system model of the galvano motor was estimated with the response behavior on the chirp signal and a 'non-linear least squares' system estimator.

As a result of the 'non-linear least squares' system estimation, the following model was obtained:

$$galvano\ motor\ model = \frac{1.242e11}{s^3 + 9517s^2 + 5.773e7s + 1.272e11}$$

Figure 4 shows the Bode plot of the measured system and the estimated model.
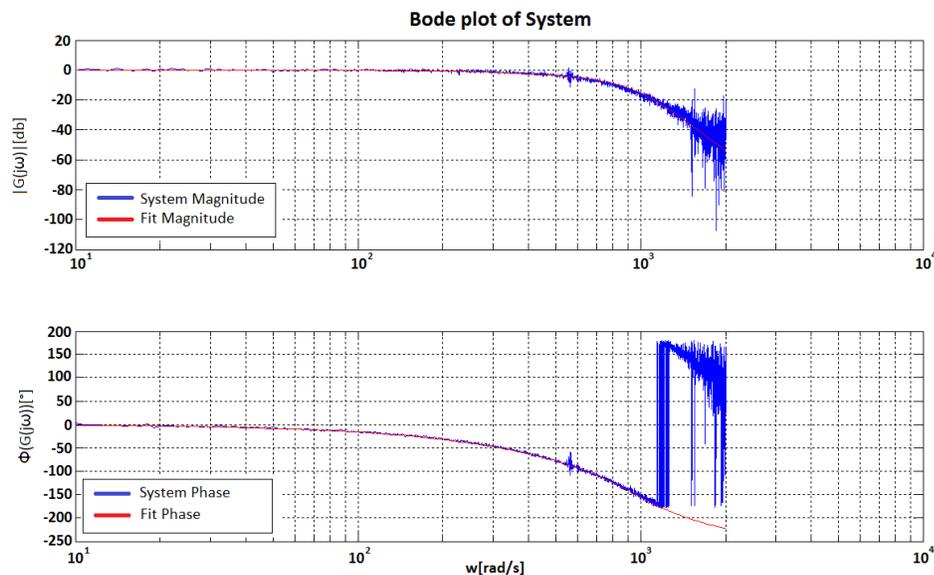
Figure 4: Bode plot of estimated galvanoscanner system

262

2. Optimal 'Input Shaper'

The system model of the galvano motor is further used in the development of the Input Shaper. The Input Shaper is developed by inverting the system model of the galvano motor. In addition, four extra poles are placed at 3000rad/s (6 times the cutoff frequency) for system stability. After this transformation the following Input Shaper was obtained:

$$Input\ shaper(continuous) = \frac{3.99e17s^3 + 3.797e21s^2 + 2.303e25s + 5.075e28}{1.272e11s^4 + 1.279e16s^3 + 4.82e20s^2 + 8.076e24s + 5.075e28}$$

$$Inpus\ shaper(discrete) = \frac{19.61z^3 - 56.99z^2 + 55.26z - 17.88}{z^4 - 3.111z^3 + 3.63z^2 - 1.882z + 0.3659}\ [fs = 1e - 5]$$

Figure 5 shows the Bode plot of the galvano motor system model, the inverted galvano motor system model and the obtained Input Shaper with four added poles for system stability.
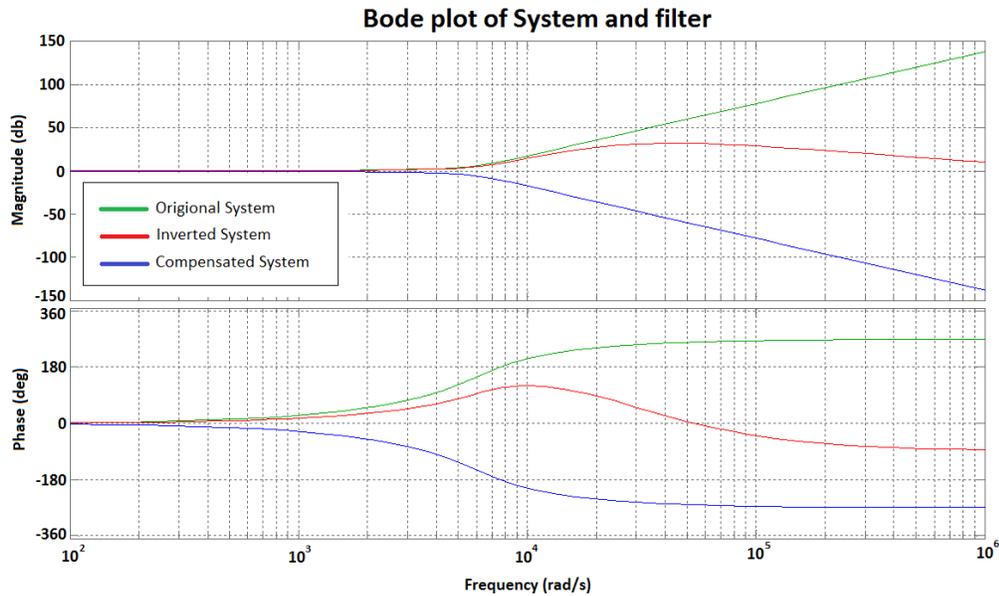
Figure 5: Bode plot of estimated galvanoscanner system, inverse of galvanoscanner system, designed input shaper

3. Validation

After the implementation of the Input Shaper, the system was validated with and without activating the Input Shaper. Figure 6 shows the response behavior (starred green line) of the galvano motor on a jump-vector (green line). When the Input Shaper is activated the jump-vector is transformed by the Input Shaper and becomes a transformed jump-vector (blue line). The response behavior on the transformed jump-vector is represented by the starred blue line. When comparing the two response behaviors, it can be noticed that both the position lag and the settling time have reduced by a factor two. Due to the reduction in position lag the jump delay can also be reduced by factor two.
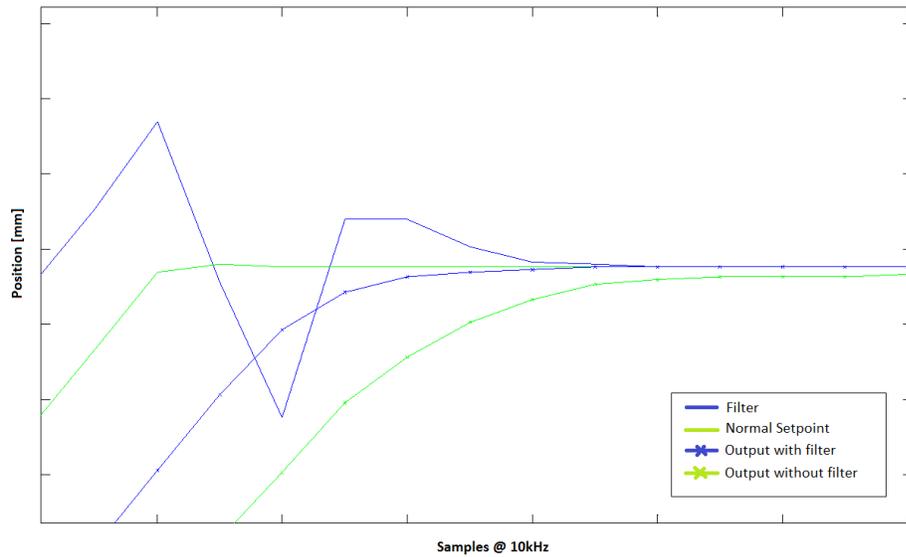
Figure 6: Position validation of the Input Shaper

Figure 7 portrays the representation of the speed response of the galvano motor with and without the activation of the Input Shaper. The blue line represents the velocity profile when the 'Input Shaper' is activated; the red line represents the velocity profile when the 'Input Shaper' is not activated. When the Input Shaper is activated, the nominal speed is achieved 25% faster.
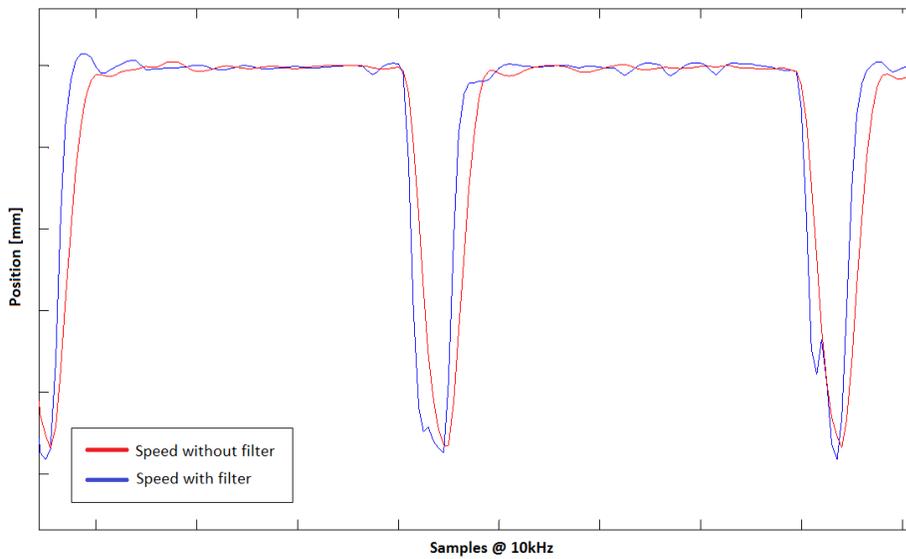
Figure 7: Speed validation of the Input Shaper

4. Test case

As test case, a lattice structured 'Stanford Bunny' [11] with open pores, a strut thickness of 250μm and a volume fraction of 5% was produced: see Figure 8. Two jobs were executed, one with and one without activation of the 'Input Shaper'. The jump-delay was reduced from 750μs to 250μs. During these jobs, the actual position of the galvano motor was logged and the total scan time was calculated. The implementation of the 'Input Shaper' results in a total scan time reduction of 10% for this lattice structured bunny, from 4686 to 4219 sec.
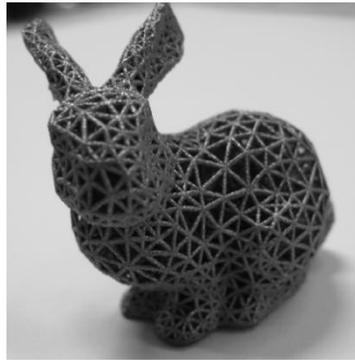
Figure 8: Test case - Porous 'Stanford Bunny' [scale 1:1]

Conclusion

The galvano scanner of KU Leuven's LM-Q SLM machine was dynamically optimized. This was done by the development and implementation of an optimal 'Input Shaper' based on the system identification of the galvano motors. Due to the higher dynamics, nominal speed can be achieved twice as fast; furthermore the 'position lag' is reduced by 50%. The greatest benefit of the optimal 'Input Shaper' is noted when manufacturing lattice structured parts. In the test case of the 'Stanford Bunny' total scanning time was reduced by 10% from 4686 sec to 4219 sec.

References

[1] J.-P. Kruth, G. Levy, F. Klocke, and T.H.C. Childs. Consolidation phenomena in laser and powder-bed based layered manufacturing, *CIRP Annals - Manufacturing Technology*, 56(2):730 − 759, 2007.

[2] L. Thijs, F. Verhaeghe, T. Craeghs, J. V. Humbeeck, and J.-P. Kruth. A study of the microstructural evolution during Selective Laser Melting of Ti-6Al-4V. *Acta Materialia*, 58(9):3303-3312,2010.

[3] J.-P. Kruth, L. Froyen, S. Kumar, M. Rombouts, and J. Van Vaerenbergh. Study of laser-sinterability of iron-based powder mixture,*10e Assises Européennes de Prototypage Rapide*, Paris, September 2004.

[5] F. Abe, K. Osakada, M. Shiomi, K. Uematsu, and M. Matsumoto. The manufacturing of hard tools from metallic powders by Selective Laser Meltin, *Journal of Materials Processing Technology*, 111(1-3):210 − 213, 2001.

[6] F. Klocke, H. Wirtz, and W. Meiners. Direct manufacturing of metal prototypes and prototype tools. *In Proceedings of the 7h Solid Freeform Fabrication symposium (SFF) 1996*, Austin (Texas - USA), August, 1996.

[7] U. Berger. Rapid tooling and Computer Tomography for aluminium casting of automotive components, *uRapid 2001 International users conference on rapid prototyping & rapid tooling & rapid manufacturing*, 2001.

[8] A. Voet, J. Dehaes, J. Mingneau, J. P. Kruth, and J. Van Vaerenbergh. Study of the wear behavior of conventional and rapid tooling mould materials, *In Int. Conf. Polymers & Moulds Innovations PMI*, Gent, Belgium, April 20-23, 2005.

[9] RTC$^®$ 5 manual, ScanLab AG - http://www.scanlab.de/en/-/products/control_boards/RTC5

[10] N.C. Singer, W.P. Seering. Preshaping Command Input to Reduce System Vibration, *Transactions of the ASME*, Vol. 112, MARCH 1990

[11] G. Turk, M. Levoy, 'Standford Bunny' − computer graphics 3D test model, Stanford University Computer Graphics Laboratory